CMIP5 Diversity in Southern Westerly Jet Projections Related to Historical Sea Ice Area: Strong Link to Strengthening and Weak Link to Shift

THOMAS J. BRACEGIRDLE

British Antarctic Survey, Cambridge, United Kingdom

PATRICK HYDER

Met Office Hadley Centre, Exeter, United Kingdom

CAROLINE R. HOLMES

British Antarctic Survey, Cambridge, United Kingdom

(Manuscript received 17 May 2017, in final form 26 September 2017)

ABSTRACT

A major feature of projected changes in Southern Hemisphere climate under future scenarios of increased greenhouse gas concentrations is the poleward shift and strengthening of the main eddy-driven belt of midlatitude, near-surface westerly winds (the westerly jet). However, there is large uncertainty in projected twenty-first-century westerly jet changes across different climate models. Here models from the World Climate Research Programme's phase 5 of the Coupled Model Intercomparison Project (CMIP5) were evaluated to assess linkages between diversity in simulated sea ice area (SIA), Antarctic amplification, and diversity in projected twenty-first-century changes in the westerly jet following the representative concentration pathway 8.5 (RCP8.5) scenario. To help disentangle cause and effect in the coupled model analysis, uncoupled atmosphere-only fixed sea surface experiments from CMIP5 were also evaluated. It is shown that across all seasons, approximately half of the variance in projected RCP8.5 jet strengthening is explained statistically by intermodel differences in simulated historical SIA, whereby CMIP5 models with larger baseline SIA exhibit more ice retreat and less jet strengthening in the future. However, links to jet shift are much weaker and are only statistically significant in austral autumn and winter. It is suggested that a significant cross-model correlation between historical jet strength and projected strength change ($r = -0.58$) is, at least in part, a result of atmospherically driven historical SIA biases, which then feed back into the atmosphere in future projections. The results emphasize that SIA appears to act in concert with proximal changes in sea surface temperature gradients in relation to model diversity in westerly jet projections.

1. Introduction

Climate models simulate a robust poleward shift and strengthening of the main eddy-driven belt of Southern Hemisphere (SH) midlatitude near-surface westerly winds (hereinafter referred to as the westerly jet or jet) under future scenarios of increased greenhouse gas concentrations (Collins et al. 2013). However, there is a large uncertainty over the magnitude of such changes across different climate models (Kidston and Gerber 2010; Wilcox et al. 2012; Bracegirdle et al. 2013; Simpson and Polvani 2016), which has global implications in terms of the rate of uptake of heat and CO_2 in the Southern Ocean (Le Quéré et al. 2007; Lovenduski et al. 2007; Frölicher et al. 2015) and ocean circulation (Hall and Visbeck 2002; Meredith and Hogg 2006; Meijers et al. 2012; Sallee et al. 2013; Waugh et al. 2013). The analysis of storm-track responses under scenarios of future anthropogenic forcing in the World Climate Research Programme's phase 5 of the Coupled Model Intercomparison Project (CMIP5) dataset (Taylor et al. 2012), conducted by Harvey et al. (2014), suggests that constraints on climate model uncertainty in polar amplification could potentially help to reduce uncertainty

Supplemental information related to this paper is available at the Journals Online website: https://doi.org/10.1175/JCLI-D-17-0320.s1.

Corresponding author: Thomas J. Bracegirdle, tjbra@bas.ac.uk

DOI: 10.1175/JCLI-D-17-0320.1

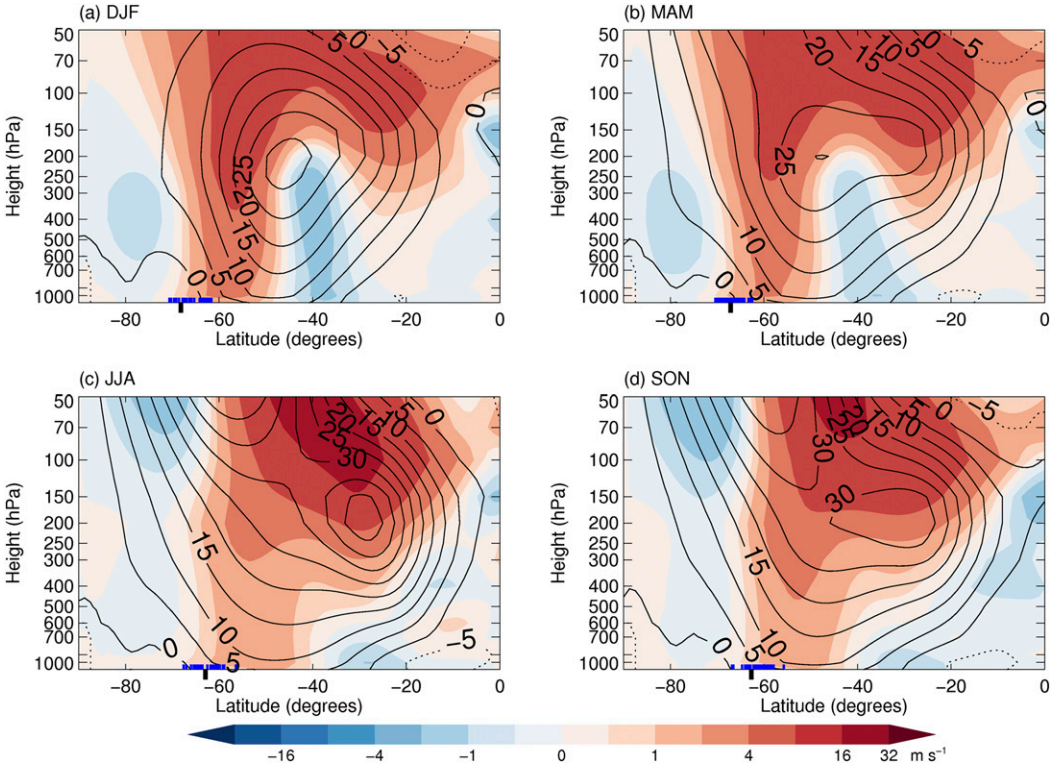

FIG. 1. Ensemble-mean twenty-first-century ΔU for (a) DJF, (b) MAM, (c) JJA, and (d) SON (color shading, with intervals 0, ±0.5, ±1, ±2, ±4, ±8, ±16, and ±32 m s^{-1}). The ensemble-mean historical climatology is shown by the contour lines (contour interval of 5 m s^{-1}). The CMIP5 historical mean sea ice edge equivalent latitudes are indicated by inward-pointing blue tick marks on the x axis (one tick mark per model), with the satellite-derived equivalent latitude shown by an outward-pointing black tick mark.

in westerly jet responses. Previous research has found that climate models with excessive SH sea ice area (SIA) in their simulations of baseline present-day climate exhibit more sea ice retreat and more Antarctic warming under scenarios of twenty-first-century increases in radiative forcing (Flato 2004; Bracegirdle et al. 2015). The link between Antarctic warming and an observable quantity (present-day SIA) therefore provides the potential to use observations to help constrain estimates of future long-term (twenty-first century) Antarctic climate change. Here this possibility is investigated in the context of the westerly jet by evaluating the degree to which model diversity in simulated SIA and related Antarctic warming may be related to model diversity in projections of change in jet position and strength in the CMIP5 models. Since the direction of causality in cross-model relationships is difficult to determine when considering just fully coupled ocean–atmosphere climate models, the potential roles of ocean–atmosphere feedbacks are assessed by comparison with atmosphere-only simulations.

By way of introduction, CMIP5 ensemble-mean-projected twenty-first-century changes in zonal mean westerly wind U and zonal mean temperature T across different seasons following the high-emission RCP8.5 scenario are shown in Figs. 1 and 2 (see section 2 for details of the data and methods). As has been documented in previous studies, under global warming scenarios midlatitude jets and storm tracks are influenced by contrasting changes in upper- and lower-tropospheric meridional temperature gradients (e.g., Held 1993; Brayshaw et al. 2011; Chavaillaz et al. 2013; Harvey et al. 2014; McGraw and Barnes 2016). In the upper troposphere, there is a broad increase in the meridional equator–pole temperature difference, as the tropics warm much more quickly than higher latitudes (Fig. 2). This acts to induce the ensemble-mean poleward shift and strengthening of the jet that is evident in Fig. 1. However, near the surface in winter there is a more rapid low-level warming at high latitudes (between approximately 60° and 70°S), which is strongest in autumn and winter in association with retreating sea ice (e.g., see Bracegirdle et al. 2008). This enhanced low-level warming is more clearly evident in austral winter (Fig. 2c) than in austral summer (Fig. 2a), broadly collocated with the range in model-simulated historical climatological ice-edge latitudes. Acting alone, more rapid polar warming

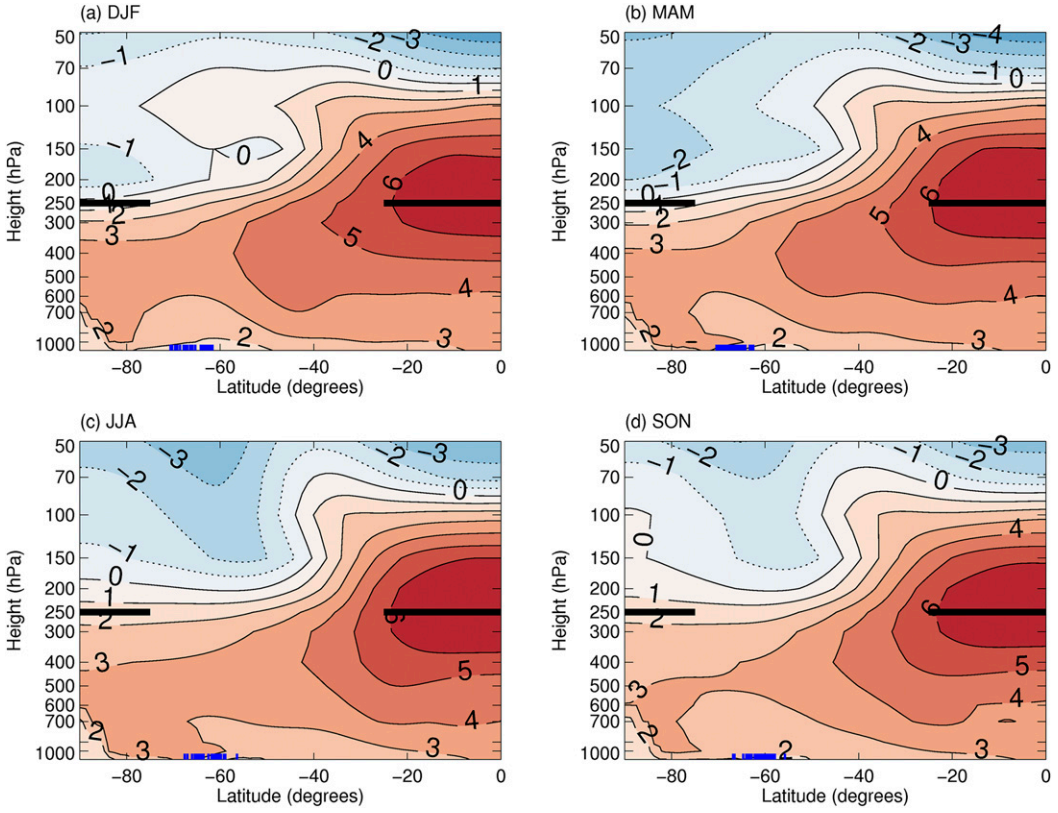

FIG. 2. As in Fig. 1, but for ΔT. The contour interval is 1 K. The horizontal solid thick black lines indicate the averaging latitudes for upper-tropospheric tropical and polar temperature, which are used to compute T_EPU.

induces a weakening and equatorward shift of the jet, therefore partially offsetting the effects of change at upper levels (e.g., Harvey et al. 2015). Although polar amplification is weaker over Antarctica than over the Arctic (in some models and seasons this ''amplification'' is less than one, but for consistency the term Antarctic amplification will still be used here), its magnitude varies significantly across different climate models, therefore potentially contributing to diversity in storm-track projections (Harvey et al. 2014).

Polar warming has been found to dominate climate model diversity in projected changes in lower-tropospheric equator–pole temperature difference (i.e., polar amplification) whereas tropical warming dominates in the upper troposphere (Chavaillaz et al. 2013; Harvey et al. 2014). Model diversity in Antarctic warming is tightly linked to change in surrounding sea surface conditions and sea ice retreat (e.g., Krinner et al. 2014; Bracegirdle et al. 2015), and in a given warming scenario, the baseline latitude of the sea ice edge affects the precise location of changes in surface meridional temperature gradient of both hemispheres (Holland and Bitz 2003). The effect of SH sea ice expansion/contraction on the westerly jet has been found to be strongest in the cold season and in configurations where retreat occurs close to the axis of the jet because of impacts on the local meridional temperature gradients (Kidston et al. 2011; Bader et al. 2013). Therefore, the simulated baseline latitude of the SH sea ice edge has the potential to modulate projected changes in the westerly jet, particularly in the cold season. It is, of course, important to point out that a number of mechanisms can induce a response in the westerly jet, such as changes in vertical temperature gradients (Frierson 2006; Yin 2005), diabatic heating (Woollings et al. 2016), tropopause height (Williams 2006; Lorenz and DeWeaver 2007), and basic state circulation change (Kushner et al. 2001; Chen and Held 2007; Wittman et al. 2007). In the CMIP5 coupled modeling framework evaluated here, all or some of these mechanisms may be operating alongside meridional temperature gradient change; therefore, again, one should take care in implying direct causality in cross-model correlations between Antarctic amplification and jet responses. However, the results of Harvey et al. (2015), where temperature gradient changes were altered directly, provide evidence for meridional temperature gradient change as a key driver.

In summer, projected changes in the westerly jet are influenced by springtime stratospheric ozone changes

over the polar cap. In the CMIP5 models, SH polar stratospheric ozone amounts recover during the twenty-first century, mainly between 2000 and 2050 (Eyring et al. 2013). Although this recovery induces a lower-stratospheric, high-latitude warming (between 100 and 200 hPa) up to 2050, under the RCP8.5 scenario the effects of greenhouse gas increases (which induce a cooling in the stratosphere) emerge to cancel out this warming during the second half of the century (Wilcox et al. 2012; see also Fig. 2d).

Model diversity in westerly jet responses to a given forcing scenario is caused by a number of factors both coupled (e.g., relating to SST and sea ice) and uncoupled (e.g., internal atmospheric dynamics). In terms of atmospheric mechanisms, previous research suggests that distinguishing between jet strength and latitude may be important both in the context of (i) internal atmospheric feedbacks and (ii) contrasting responses to different external drivers. Regarding the first point, the widely reported state dependency between simulated baseline jet latitude and diversity in poleward shifts across different climate models has been suggested to be due to internal atmospheric dynamical processes such as coherence of eddy feedbacks (Simpson et al. 2012) and fluctuation–dissipation theory (Kidston and Gerber 2010; McGraw and Barnes 2016). However, McGraw and Barnes (2016) found no clear state dependency in jet strength and attributed this to a weaker fluctuation–dissipation effect for strength. On the second point, upper-level meridional temperature gradient changes have been found in a range of model setups to have more impact on westerly jet shift compared to lower-level and/or surface meridional temperature gradient changes (Riviere 2011; McGraw and Barnes 2016). Previous studies of links between diversity in CMIP responses of the westerly jet to climate forcing have focused mainly on jet shift, thus motivating an analysis of both shift and strength change here.

In this study the CMIP5 dataset is used to answer the following questions:

1) How strong are the cross-model relationships between historical SIA, Antarctic amplification, and projected twenty-first-century changes in strength and position of the westerly jet?
2) How strong is the evidence for a direct influence of sea ice retreat on diversity in jet projections?
3) What is the potential role of internal atmospheric feedbacks in driving diversity in sea ice and jet projections (and their linkages)?

2. Data and methods

The CMIP5 dataset was used for the analysis in this study. Data from two of the fully coupled experiments were used: historical and representative concentration pathway 8.5 (RCP8.5). Both the historical and RCP8.5 coupled simulations are forced by known important anthropogenic and natural drivers of climate change (Meinshausen et al. 2011). In addition, data from four atmosphere-only experiments with fixed sea surface temperature (SST) and sea ice were also used (amip, amipFuture, amip4K, and amip4xCO2). For amip, the lower boundary SST and sea ice are prescribed based on time-varying observations from 1979 to 2008, along with the same natural and anthropogenic atmospheric climate forcings that were used in the historical experiment. In amipFuture, a patterned forcing of projected future SST change is added to the amip experimental setup, which is otherwise unchanged. CMIP3 simulations are used to define the SST warming pattern, which is scaled such that the global mean SST forcing is 4 K. The same approach is used for the amip4K experiments, except that a uniform SST warming of 4 K is added rather than a patterned warming. In both amipFuture and amip4K, sea ice is kept at control (amip) values. In the amip4xCO2 experiment, atmospheric CO_2 concentrations were quadrupled relative to preindustrial levels, but with the same surface conditions as amip.

For analysis of the coupled historical and RCP8.5 simulations, diagnostics were derived from annual and seasonal means of multiannual climatologies of monthly mean CMIP5 data: zonal wind on pressure levels (CMIP5 variable name ua), temperature on pressure levels (ta), air temperature at 2 m (tas), and sea ice concentration (sic). The 30-yr climatological means for each month were calculated for both the late twentieth century (1970–99) from the historical data and the late twenty-first century (2070–99) from the RCP8.5 data. Twenty-first-century responses to anthropogenic forcing were calculated as differences between the late-twenty-first century (RCP8.5) and late-twentieth-century (historical) climatologies.

Although the 1970–99 baseline period could potentially be affected by rapid loss of SH polar stratospheric ozone from the late 1970s, the results were not found to be sensitive to the use of an earlier baseline period (1870–99). For analysis of the amip simulations, only monthly zonal wind on pressure levels (ua) was required. The climatologies for each month were used to produce seasonal and annual climatologies, which were then used to calculate the westerly jet, temperature, and sea ice diagnostics. The required data were found for 36 CMIP5 models, with a subset of 25 available from the amip simulations and 12 available from the amipFuture, amip4K, and amip4xCO2 simulations (Table 1). For some models, data were available from multiple realizations of the same experiment (see Tables S1–S3 in the supplemental material). In these cases, the time-slice

TABLE 1. Models used and modeling center from historical and RCP8.5 simulations are listed in the first two columns. The amip, amipFuture, amip4xCO2, and amip4K subsets are indicated in the remaining columns. See the appendix for expansion of modeling center acronyms and https://www.ametsoc.org/PubsAcronymList for expansions of model name acronyms.

Model names for historical and RCP8.5	Modeling center	amip	amipFuture	amip4xCO2	amip4K
ACCESS1.0	CSIRO–BoM	x			
ACCESS1.3	CSIRO–BoM	x			
BCC_CSM1.1	BCC	x	x	x	x
BCC_CSM1.1(m)	BCC	x			
BNU-ESM	GCESS	x			
CanESM2	CCCma	x[a]	x[a]	x[a]	x[a]
CCSM4	NCAR	x	x		x
CESM1(BGC)	NSF–DOE–NCAR				
CESM1(CAM5)	NSF–DOE–NCAR	x	x		
CESM1(WACCM)	NSF–DOE–NCAR				
CMCC-CM	CMCC	x			
CMCC-CMS	CMCC				
CNRM-CM5	CNRM–CERFACS	x	x	x	x
CSIRO Mk3.6.0	CSIRO–QCCCE	x			
EC-EARTH	EC-EARTH	x			
FGOALS-g2.0	LASG–CESS	x		x	x
FIO-ESM	FIO				
GFDL CM3	NOAA/GFDL	x			
GFDL-ESM2G	NOAA/GFDL				
GFDL-ESM2M	NOAA/GFDL				
GISS-E2-H	NASA GISS				
GISS-E2-R	NASA GISS	x			
HadGEM2-AO	NIMR/KMA				
HadGEM2-CC	MOHC				
HadGEM2-ES	MOHC	x[b]	x[b]	x[b]	x[b]
INM-CM4.0	INM	x			
IPSL-CM5A-LR	IPSL	x	x	x	x
IPSL-CM5A-MR	IPSL	x			
IPSL-CM5B-LR	IPSL	x	x	x	x
MIROC-ESM-CHEM	MIROC				
MIROC5	MIROC	x	x	x	x
MPI-ESM-LR	MPI-M	x	x	x	x
MPI-ESM-MR	MPI-M	x	x	x	x
MRI-CGCM3	MRI	x	x	x	x
NorESM1-M	NCC	x		x	
NorESM1-ME	NCC				

[a] Atmosphere-only model, CanAM4.
[b] Atmosphere-only model, HadGEM2-A.

climatologies for each model were calculated from means across the available realizations for that model. The purpose of using all available realizations was to minimize the impact of internal climate variability on the results. A check of the sensitivity of results to using just a single realization from each model showed only a negligible impact on the results (not shown).

Estimates of actual late-twentieth-century westerly winds were taken from the observationally constrained European Centre for Medium-Range Weather Forecasts (ECMWF) interim reanalysis (ERA-Interim) dataset (Dee et al. 2011).

The westerly jet diagnostics were calculated from zonally averaged zonal wind climatologies at 850 hPa (seasonal and annual means as described above). A cubic spline interpolation was first used to interpolate onto a latitudinal grid with intervals of 0.075°, which is approximately one order of magnitude smaller than the lower end of the range in latitudinal grid spacing used across the CMIP5 models. The maximum between the latitudes of 75° and 10°S was then identified and used to define the jet position (latitude) and strength denoted as JPOS and JSTR, respectively. Twenty-first-century change (or response), denoted ΔJPOS and ΔJSTR, was defined as differences between jet diagnostics calculated from the late-twenty-first-century RCP8.5 climatologies and late-twentieth-century historical climatologies.

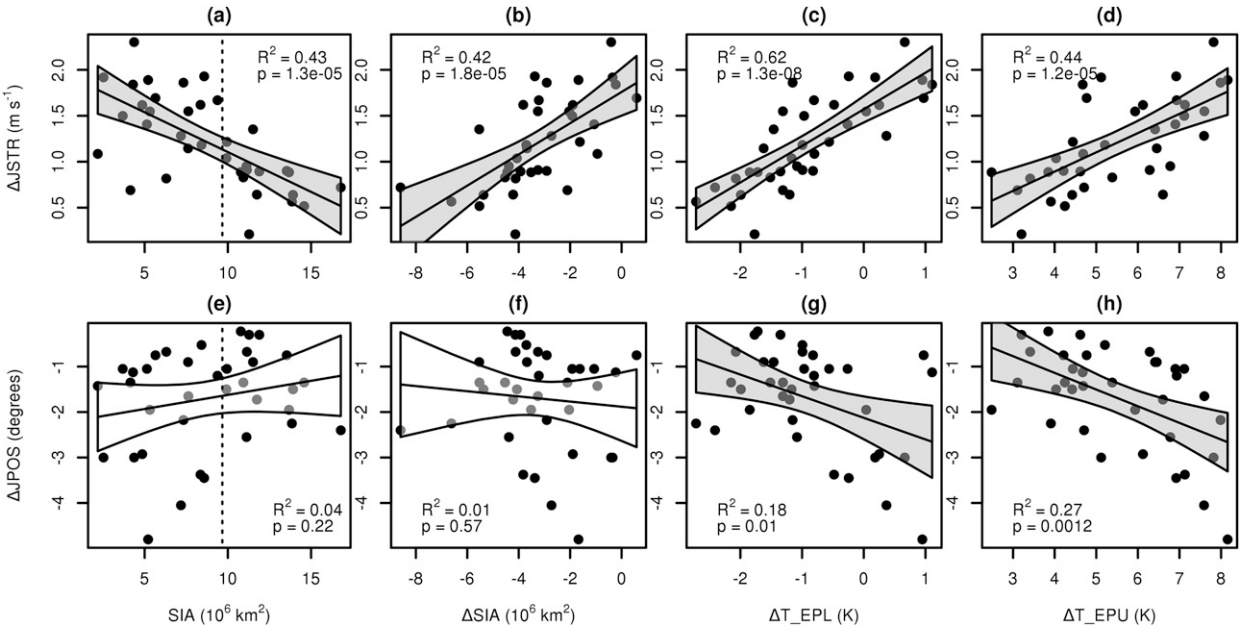

FIG. 3. Scatterplots of SIA, ΔSIA, Δ*T*_EPL, and Δ*T*_EPU vs twenty-first-century change in (a)–(d) JSTR and (e)–(h) JPOS. Each dot represents a CMIP5 model. Linear regression best fit lines and 95% confidence intervals are shown in each panel. Gray shading indicates $p < 0.05$ based on the two-tailed Student's t test. The vertical dashed lines in (a) and (e) indicate a satellite-based estimate of historical annual-mean SIA (1979–99) from the NASA Bootstrap 2 sea ice concentration dataset (Comiso 2000). The variance explained R^2 and p values are additionally displayed in each panel.

Sea ice area was defined as the area integral of Southern Hemisphere seasonal and annual-mean sea ice concentration. The historical mean and twenty-first-century response (following the RCP8.5 scenario) in sea ice area are, as for the jet diagnostics, denoted as SIA and ΔSIA, respectively. A comparison with results based on sea ice extent (SIE) in place of SIA showed highly correlated results in terms of intermodel diversity in projected responses (the cross-model correlation between annual-mean ΔSIA and ΔSIE was found to be 0.99). For SIE, annual and seasonal means were necessarily compiled from extent calculations in each month separately, for which the extent was calculated as the area enclosed by the 15% concentration threshold (e.g., Comiso 2000). A sea ice edge "equivalent latitude" diagnostic was also calculated for comparison on relevant zonal cross-section plots. This follows the approach of Eisenman (2010) by first defining an equivalent extent as the sum of SIE and the area of the Antarctic continent, which is then proportional to the sine of the latitude of the sea ice edge. The CMIP5 land area fraction fields (CMIP5 variable sftlf) were used to calculate the area of the Antarctic continent as defined in each model.

Seasonal and annual mean climatologies of zonally averaged air temperature were used to calculate upper (250 hPa) and lower [near-surface (2 m)] SH equator–pole temperature differences (denoted as *T*_EPU and *T*_EPL, respectively, with their twenty-first-century change expressed as Δ*T*_EPU and Δ*T*_EPL). Latitude ranges of 90°–75°S and 25°S–0° were used for polar and equator temperature diagnostics, respectively.

Polar amplification was defined as the ratio between polar cap 2-m temperature RCP8.5 twenty-first-century response (area-weighted mean poleward of 60°S) and globally averaged 2-m temperature response. As might be expected, Δ*T*_EPL is highly anticorrelated with Antarctic amplification across the CMIP5 models ($r = -0.95$ for annual mean quantities).

3. Results

a. *Sea ice area, meridional temperature gradients, and diversity in westerly jet projections*

The initial results presented are annual mean quantities, since they capture the main qualitative picture that is broadly seen across the different seasons evaluated below. In Fig. 3 cross-model relationships between projected changes in the westerly jet and upper and surface equator–pole temperature differences are shown along with SIA and ΔSIA (which are highly correlated with each other, $r = -0.83$). The main feature evident from Fig. 3 is that the surface parameters (SIA, ΔSIA, and Δ*T*_EPL) are much more strongly related to

TABLE 2. Linear regression variances explained and sign of slopes ($|r|r$) for the variables shown in Fig. 3, but for different seasons. p values of less than 0.01 are indicated by boldface font, $0.01 \leq p < 0.05$ by italic font, and $p \geq 0.05$ by normal roman font.

	DJF		MAM		JJA		SON	
	ΔJSTR	ΔJPOS	ΔJSTR	ΔJPOS	ΔJSTR	ΔJPOS	ΔJSTR	ΔJPOS
SIA	**−0.39**	0.10	**−0.58**	**0.20**	**−0.29**	**0.20**	**−0.24**	0.01
ΔSIA	**0.29**	−0.08	**0.54**	−0.10	**0.37**	−0.12	**0.23**	0.00
Δ*T*_EPL	**0.58**	**−0.37**	**0.53**	*−0.16*	**0.54**	−0.16	**0.65**	*−0.17*
Δ*T*_EPU	**0.50**	**−0.66**	**0.43**	**−0.39**	**0.46**	**−0.18**	**0.40**	*−0.17*

ΔJSTR than to ΔJPOS across the models. The contrast is clearest for SIA and ΔSIA, for which nearly half of the variance in jet strength projections is explained (43% and 42%, respectively; Figs. 3a,b), and yet only 4% and 1% is explained for diversity in jet shift projections (Figs. 3e,f). In contrast, Δ*T*_EPU exhibits significant cross-model relationships with both jet shift and strength change.

In Table 2 the relationships shown in Fig. 3 are extended to all four canonical seasons. The seasonal results are qualitatively similar to the annual mean results. Significant relationships between jet strength and SIA are evident in all seasons. The largest explained variances involving sea ice are in autumn (MAM) (as large as 58% for jet strength change regressed onto SIA). There is also a statistically significant relationship between jet shift and SIA in autumn, although this is much weaker and explains only 20% of the intermodel variance. The statistically significant slopes in regressions of jet strength onto sea ice variables in DJF serve as a reminder that cause and effect cannot be implied by the cross-model relationships alone, since changes in sea ice in summer are small and have been found in atmosphere-only studies to have a negligible effect on tropospheric circulation (e.g., Raphael 2003; Kidston et al. 2011). Other aspects of the climate system will change along with sea ice in a coupled model setup; therefore, to provide a broader picture of wider linkages, Fig. 4 shows latitude–height cross sections

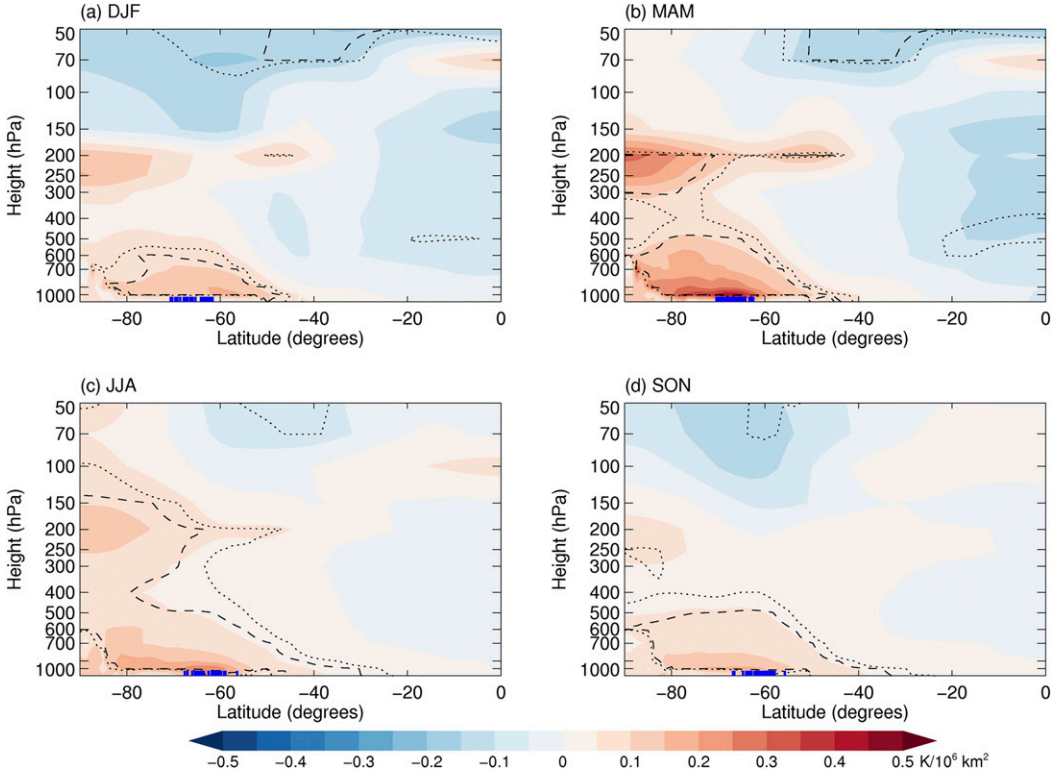

FIG. 4. Slopes of CMIP5 twenty-first-century Δ*T* linearly regressed onto simulated historical SIA for (a) DJF, (b) MAM, (c) JJA, and (d) SON. The dotted and dashed lines bound regions of statistical significance at the $p = 0.05$ and 0.01 levels, respectively, based on the two-sided Student's *t* test. As in Fig. 1, the CMIP5 historical mean sea ice edge equivalent latitudes are indicated by blue inward-pointing tick marks on the *x* axis.

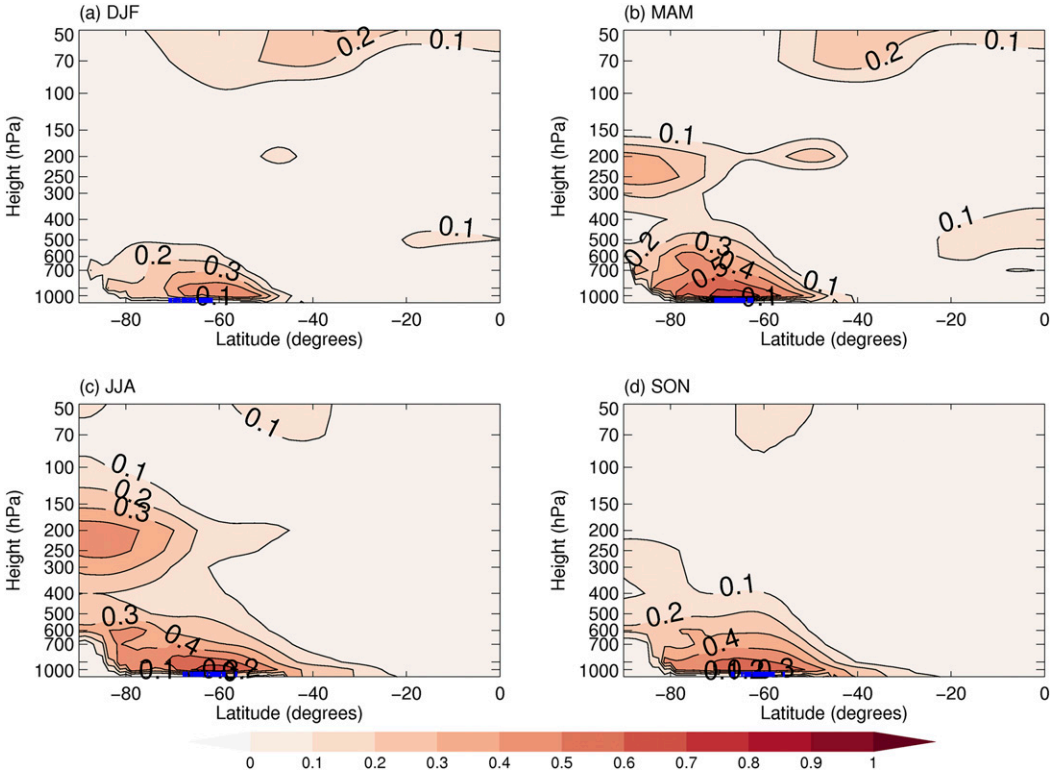

FIG. 5. As in Fig. 4, but for R^2.

of cross-model regressions of projected zonal mean temperature response ΔT onto historical SIA.

Figure 4 shows that, as described previously in Bracegirdle et al. (2015), CMIP5 models with more extensive sea ice in their historical climatologies exhibit more high-latitude, low-level warming associated with larger projected loss of sea ice in these models. In summer (DJF), the region of significant near-surface regression slopes extends to approximately 50°S (Fig. 4a), which is equatorward of the multimodel mean summer equivalent sea ice edge close to the Antarctic coastline at approximately 65°S. Although the multimodel mean and observed sea ice areas are small in summer, it is clear from Fig. 1a that some models exhibit relatively large summer ice areas. This helps to explain the existence of statistically significant temperature–SIA relationships in summer, although overall this region of significant regression slopes (bounded by the dashed lines in Fig. 4a) is small and largely confined to high latitudes and low altitudes.

Autumn (MAM) and winter (JJA) are the seasons with the most extensive and significant linear relationships between ΔT and SIA (Figs. 4b,c and 5b,c) and ΔSIA (not shown). This is consistent with the larger projected future surface temperature responses in regions of ice retreat in MAM and JJA compared to SON and DJF (Bracegirdle et al. 2008). As noted in Bracegirdle et al. (2015), in all seasons the high-latitude temperature changes are not significantly related to low-latitude change across the different CMIP5 models (implying that models with a larger retreat of sea ice and stronger polar warming do not necessarily exhibit larger tropical warming, and vice versa). It therefore appears that processes at mid-to-high southern latitudes are the key to constraining model uncertainty in the rate of warming at high southern latitudes.

The latitude–height cross sections of zonal mean zonal wind response ΔU regressed onto SIA also show more significant relationships in MAM and JJA compared to SON and DJF as expected (Figs. 6 and 7), with larger regions of significant slopes and larger associated explained variances. Indeed, up to approximately one-third of the intermodel variance in lower-tropospheric ΔU at mid-to-high latitudes can be explained statistically by historical sea ice area. This is lower than the explained variances for jet strength change regressed onto SIA (Fig. 3 and Table 2), which is likely a consequence of differing latitudes of the jet across different CMIP5 models.

One of the implications of the results shown in Fig. 3 and Table 2 is that constraining projections of relative Antarctic warming (Antarctic amplification) in the

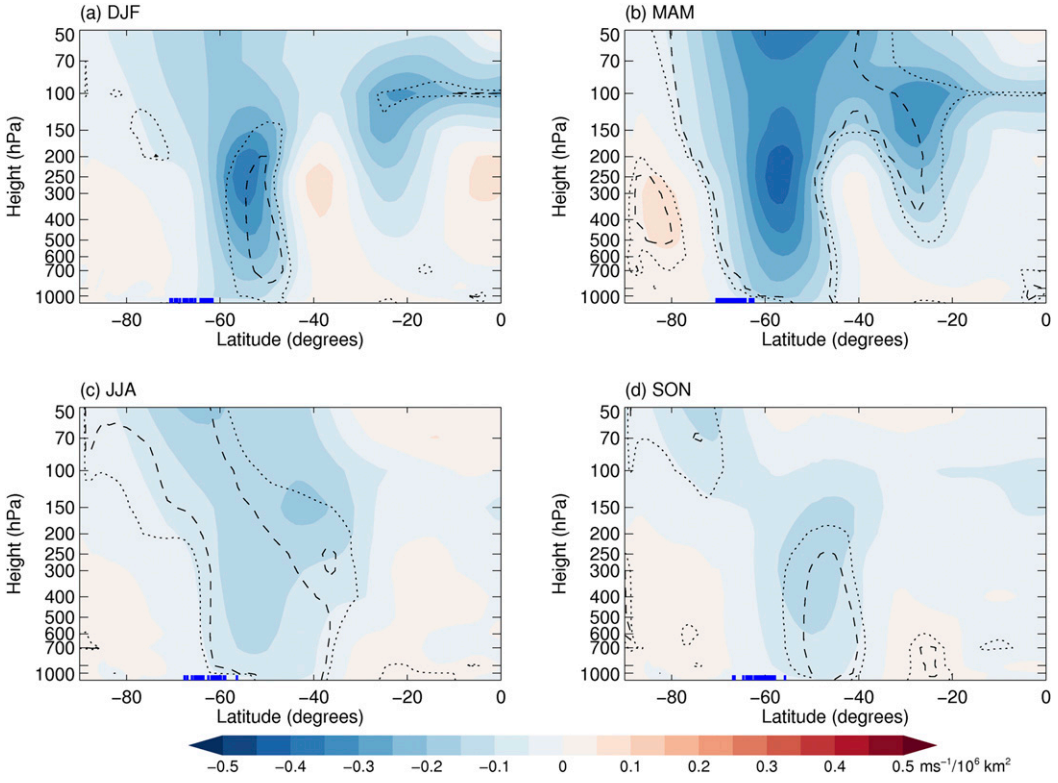

FIG. 6. As in Fig. 4, but for twenty-first-century ΔU linearly regressed on historical SIA.

CMIP5 ensemble is of more importance with regard to diversity in projections of jet strength than jet latitude. To investigate this further, Fig. 8 shows projected ΔT regressed onto ΔJSTR (Figs. 8a,b) and ΔJPOS (Figs. 8c,d). The most striking feature of Fig. 8 is that the region of large regression slopes near the surface at high latitudes associated with ΔJSTR (poleward of ~50°S in Figs. 8a,b) is almost completely absent in regressions of ΔT onto ΔJPOS (Figs. 8c,d). Also consistent with Fig. 3, model diversity in upper-tropospheric tropical warming is related to both jet shift and strengthening (Figs. 8a,c).

b. *Comparing model diversity in historical bias and response across AMIP and CMIP*

The direction of causality is not clear from the cross-model relationships shown in the previous subsection. One way to investigate this is to compare model diversity across different variables in coupled (historical and RCP8.5) and uncoupled atmosphere-only simulations (amip, amipFuture, amip4K, and amip4xCO2), which represents an extension of the approach of Hyder et al. 2017 (manuscript submitted to *Nat. Commun.*) to include future response. Since the SST and sea ice fields do not vary between models in the amip-style experiments, the baseline amip jet biases and inter-model diversity in jet responses will be independent of ocean–atmosphere–ice feedbacks. For simplicity, the discussion of the amip perturbation results below is primarily focused on the results from amipFuture. The amip4K and amip4xCO2 results are shown in Table S3 of the supplemental material to evaluate robustness of the amipFuture results.

One possibility is that the intrinsic atmospheric baseline JSTR could play a key role in setting the baseline historical SIA and therefore influence ΔSIA by, at the simplest level, varying the amount of sea ice available to retreat (and induce lower-tropospheric warming) in the future. Mahlstein et al. (2013) showed that there is a strong relationship between near-surface westerlies over the Southern Ocean (south of 55°S) and SIA across the CMIP5 models in all seasons. Similarly, significant links are seen here between annual-mean JSTR and SIA (Fig. 9a) in coupled simulations, which are consistently statistically significant across all four seasons (not shown). However, it is not clear whether SIA biases and/or correlated variables (e.g., SST gradients) are driving the atmospheric biases, or vice versa. Figure 9 indicates a significant role for intrinsic atmospheric biases, whereby models with a strong jet in coupled mode also exhibit a strong jet in atmosphere-only (amip) mode (Fig. 9b); as a consequence, coupled SIA biases are positively correlated with amip jet

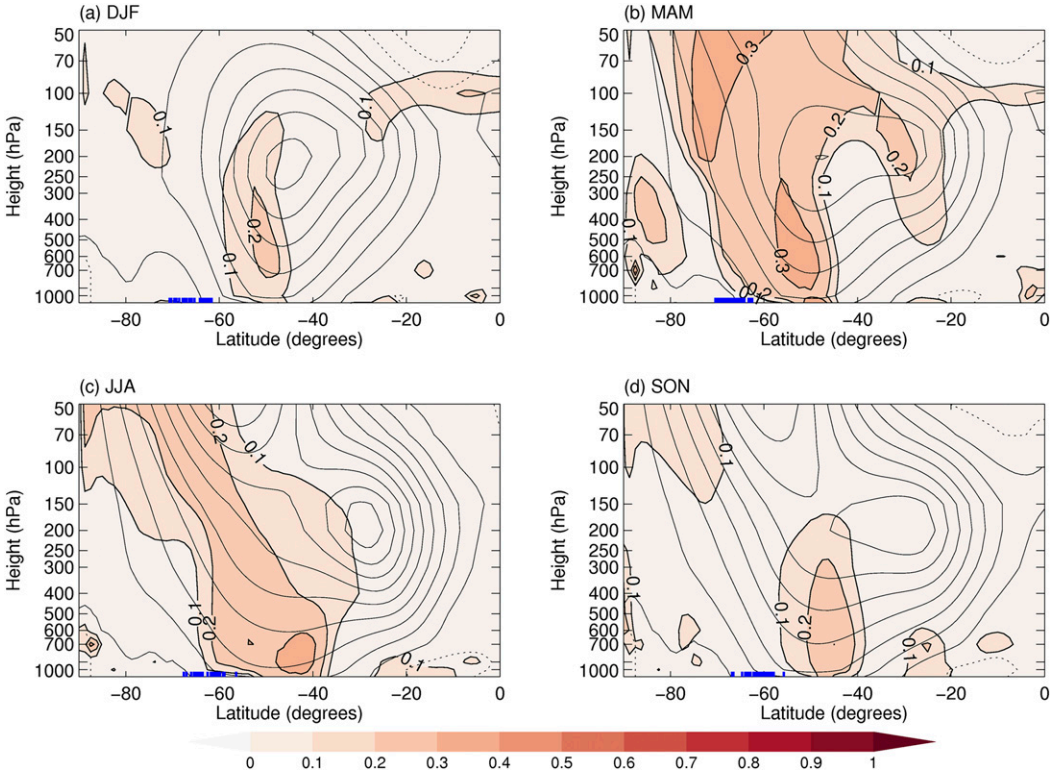

FIG. 7. As in Fig. 6, but for R^2. In addition, the ensemble-mean historical climatology of U is shown by the thin contour lines (repeated from Fig. 1 to aid comparison with regression patterns).

strength biases (Fig. 9c). In other words, this is consistent with a significant role for intrinsic atmospheric jet strength as a driver of intermodel differences in coupled historical SIA. Observational estimates lie within the 95% confidence interval of the linear fit between historical jet strength and SIA (Fig. 9a), indicating that models with more realistic jet strength also broadly exhibit a more realistic SIA. No significant relationships were found when this analysis was repeated for jet latitude (not shown).

It is natural then to ask the extent to which model diversity in projected SIA retreat (or ΔSIA) may also have been driven by intermodel differences in intrinsic atmosphere-only westerly jet responses. If internal atmospheric responses to greenhouse gas forcing (and associated SST change) are a significant driver of diversity in sea ice responses across the different models, then one might expect that models with more jet strengthening in atmosphere-only mode would also exhibit more jet strengthening in coupled mode and less retreat of sea ice. However, this was not found to be the case (Fig. 10): no significant correlations were found between diversity in amipFuture responses and jet strength responses in coupled CMIP5 simulations with common atmospheric components (see Table 1). (Note that this result is not changed if Fig. 10 is repeated based on responses from amip4xCO2 or amip4K; see Figs. S1 and S2 in the supplemental material.) This implies that ocean/ice surface changes (or atmosphere–ice–ocean interactions) are key to determining the diversity in coupled CMIP5 ΔJSTR.

Consistent with the possibility of an important role for ocean–ice–atmosphere feedbacks in driving diversity in ΔJSTR, a negative cross-model correlation evident in the CMIP5 models between historical JSTR and RCP8.5 response (ΔJSTR; $r = -0.58$, expressed as $|r|r = -0.33$ in Table 3, for annual mean parameters) is entirely absent from a comparative assessment of amip baseline jet strength versus amipFuture responses (Table 3). In contrast, the well-established jet latitude state dependence still persists in winter (JJA) for amipFuture and amip4K responses and spring (SON) and autumn (MAM) for amip4xCO2 responses (Tables 3 and 4). This is consistent with the weaker correlations between jet latitude and SIA documented earlier in this paper and the internal atmospheric mechanisms discussed in the introduction.

The broader picture, therefore, appears to be that intrinsic intermodel differences in jet strength simulated in atmosphere-only mode play a key role in driving diversity in coupled historical SIA, but that surface changes and/or coupled feedbacks are the main driver of diversity in coupled RCP8.5 jet strength responses.

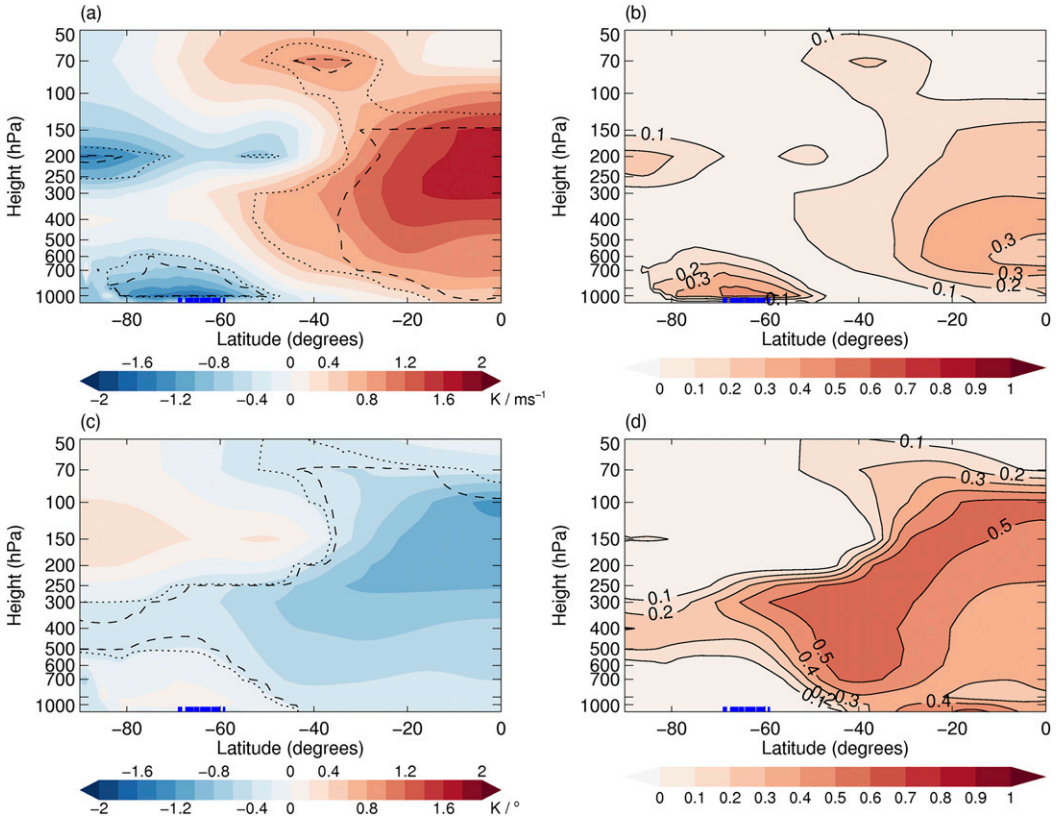

FIG. 8. The ΔT regressed onto (top) ΔJSTR and (bottom) ΔJPOS for (a),(c) linear regression slopes and (b),(d) R^2.

Therefore, this provides a mechanism by which the existence of, for example, a weak historical westerly jet in a given model (and resulting smaller SIA) could cause the same model to exhibit stronger future strengthening under increased greenhouse gases (since less ice is available to retreat in the future).

4. Conclusions

In this study, relationships across different CMIP5 models between SH SIA, equator–pole meridional temperature gradients (Antarctic amplification), and the SH tropospheric westerly jet have been examined. This was

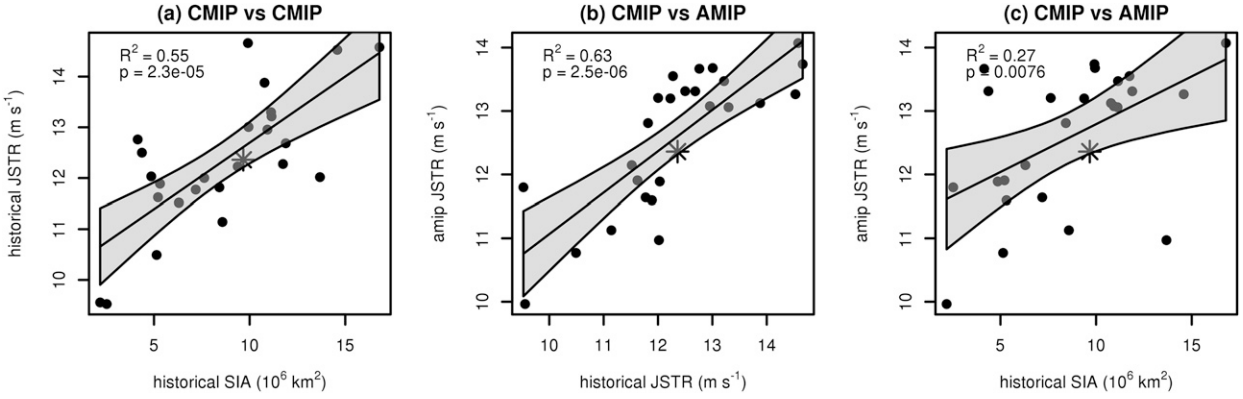

FIG. 9. Scatterplots of (a) historical SIA vs historical JSTR, (b) historical JSTR vs amip JSTR, and (c) historical SIA vs amip JSTR. A subset of 25 models is shown for which corresponding atmospheric components are available across both amip and coupled CMIP5 models (Table 1). The asterisks show observational estimates of the quantities plotted, specifically satellite-estimated annual-mean SIA vs reanalysis-based annual-mean JSTR for the period 1979–99 (NASA Bootstrap 2 and ERA-Interim). The linear regression lines and symbols follow Fig. 3. The best fit lines and confidence intervals follow the definitions in Fig. 3.

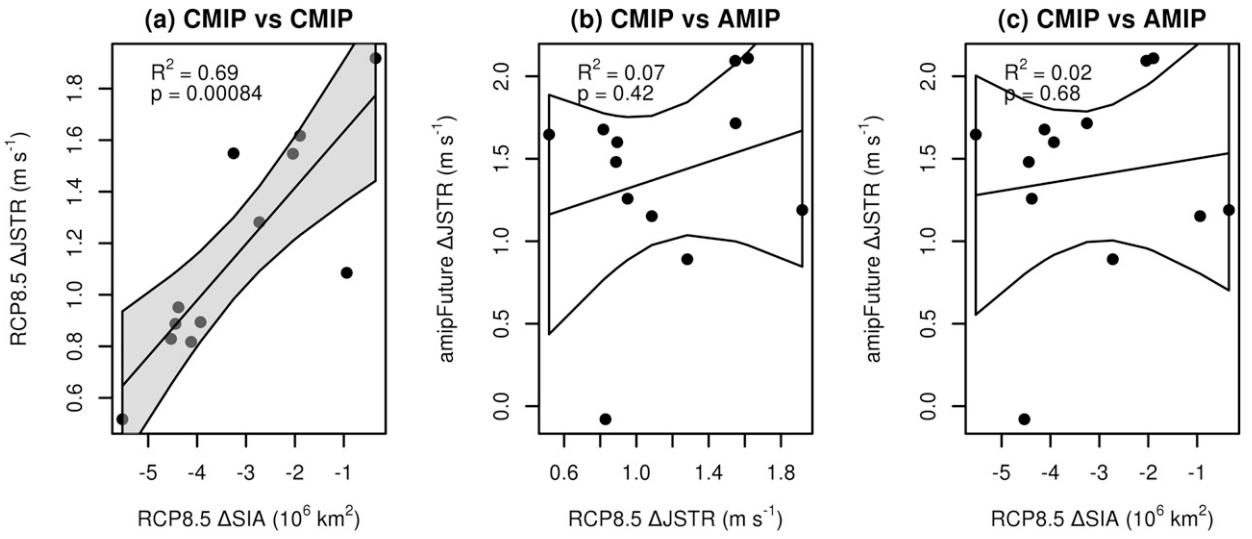

FIG. 10. (a) As in Fig. 3b, but for a subset of the 12 coupled CMIP5 simulations for which corresponding atmospheric components are available across both amip and amipFuture (see Table 1); (b) As in (a), but for coupled RCP8.5 ΔJSTR vs amipFuture ΔJSTR. (c) As in (a), but for RCP8.5 ΔSIA vs amipFuture ΔJSTR.

motivated by previous results showing that CMIP5 models with excessive SIA in their historical simulations exhibit more retreat of sea ice and stronger Antarctic warming in their future projections. The aim of this study was to determine the degree to which future projections of strength and position of the westerly jet may also be related to intermodel diversity in simulated SIA.

Here we answer the questions posed in the introduction:

1) Projected future change in the westerly jet is strongly related across the CMIP5 models with simulated historical SIA, ΔSIA, and ΔT_EPL. Across all seasons approximately half of the variance in projected jet strengthening is explained statistically by simulated SIA (R^2 as high as 0.58 in MAM), whereby models with larger historical SIA exhibit less strengthening in the future. However, links between SIA and jet shift are much weaker and only statistically significant in MAM and JJA (see Table 2). Indeed, diversity in jet shift projections is more strongly related to tropical warming and ΔT_EPU.
2) The stronger correlations between SIA and the westerly jet in MAM and JJA are consistent with a stronger direct effect of sea ice retreat in those seasons. However, the results emphasize that SIA likely acts in concert with proximal high-latitude changes in sea surface temperature gradients and that the SIA diagnostic in the context of cross-model correlations should therefore be considered as representing these combined effects. Further research is required to elucidate the interactions and feedbacks of different components of the atmosphere–ocean–ice system around Antarctica.
3) No clear evidence was found to support the possibility that intermodel differences in the intrinsic atmosphere-only jet responses are the main driver of diversity in coupled CMIP5 SIA responses (i.e., ΔSIA). However, the results suggest that historical biases in jet strength could feed back onto jet strength projections by influencing historical SIA and therefore the amount of ice available to retreat in the future.

TABLE 3. Regression variances explained and sign of slopes ($|r|r$) for cross-model correlations between baseline and forcing response in JSTR and JPOS. Statistical significance is indicated as in Table 2.

	Historical, RCP8.5 (n = 36)		amip, amipFuture (n = 12)	
	JSTR, ΔJSTR	JPOS, ΔJPOS	JSTR, ΔJSTR	JPOS, ΔJPOS
Annual	**−0.33**	**−0.40**	0.00	−0.23
DJF	**−0.26**	*−0.14*	0.00	0.09
MAM	**−0.33**	**−0.29**	−0.08	**−0.54**
JJA	**−0.26**	**−0.69**	0.00	**−0.51**
SON	**−0.22**	**−0.35**	0.00	0.00

TABLE 4. As in Table 3, but for amip4xCO2 and amip4K responses. Statistical significance is indicated as in Table 2.

	amip, amip4xCO2 (n = 12)		amip, amip4K (n = 12)	
	JSTR, ΔJSTR	JPOS, ΔJPOS	JSTR, ΔJSTR	JPOS, ΔJPOS
Annual	0.06	−0.27	0.00	−0.24
DJF	−0.05	−0.15	−0.24	0.03
MAM	0.02	*−0.34*	−0.06	−0.20
JJA	0.01	−0.15	0.08	**−0.52**
SON	−0.02	*−0.41*	0.12	−0.02

5. Discussion

In evaluating diversity in jet responses and Antarctic amplification, an important consideration is that, as has been noted previously (Chavaillaz et al. 2013; Bracegirdle et al. 2015), CMIP5 models with a large tropical (and indeed global) transient twenty-first-century warming do not necessarily exhibit a large surface warming at southern high latitudes. A key consequence of this is that Antarctic amplification is highly correlated with both absolute projected Antarctic warming and ΔSIA (r = 0.90 and −0.88, respectively, for annual mean quantities). Therefore, in a qualitative sense, Antarctic amplification, absolute Antarctic warming, and ΔSIA may be considered as interchangeable across the CMIP5 models. This is relevant to projections of the westerly jet, for which changes in the meridional temperature gradient associated with Antarctic amplification are of key importance. It is notable that this contrasts with the Arctic, where Arctic amplification is less strongly correlated with absolute Arctic warming and sea ice area change (r = 0.63 and −0.56, respectively, for the 36 CMIP5 models assessed here) and absolute near-surface (2 m) warming is more strongly correlated with global warming (r = 0.81, which compares to r = 0.40 for Antarctic vs global warming). The implication is that efforts to observationally constrain uncertainty in Antarctic amplification (at least in the CMIP5 models) are analogous to constraining absolute Antarctic warming, whereas over the Arctic one needs to consider regional warming relative to lower latitudes.

As a consequence of this close cross-model association between Antarctic amplification and sea ice change, Antarctic sea ice responses are strongly correlated with SH responses in lower-tropospheric meridional temperature gradient and therefore highly relevant to uncertainty in responses of the westerly jet. Our results are in agreement with previous studies showing that diversity in multimodel projections of SH jet shift is strongly related to equator–pole meridional temperature gradients in both the upper and lower troposphere (Wilcox et al. 2012; Gerber and Son 2014; Harvey et al. 2014; Grise and Polvani 2016). In agreement with Grise and Polvani (2016), we find that intermodel diversity in projected jet shift is not strongly related to sea ice. Rather, for the twenty-first-century period and scenario evaluated here, jet strength was found to be much more strongly related to SIA than jet latitude. Therefore, although sea ice has been found to induce jet shifts in idealized numerical experiments (e.g., Kidston et al. 2011; Bader et al. 2013; Sime et al. 2013), other factors appear to dominate model uncertainty in jet shift in the fully coupled global change scenarios evaluated here. Recent studies based on simplified modeling frameworks provide a possible explanation of the stronger cross-model link between SIA and jet strength compared to latitude. Both McGraw and Barnes (2016) and Baker et al. (2017) show that low-level, high-latitude heating anomalies in dry dynamical models induce a more consistent impact on jet strength than jet latitude across a range of model configurations [different baseline jet latitudes in McGraw and Barnes (2016) and different latitudes of maximum heating in Baker et al. (2017)]. It should be noted that studies of paleoclimate simulations show a stronger cross-model link between sea ice (and polar amplification) and uncertainty in jet shift when comparing the Last Glacial Maximum (LGM) and preindustrial climate conditions. It is suggested that this can be explained by the greater importance of polar temperature changes in model diversity in equator–pole temperature gradient changes between the LGM and preindustrial period and the closer proximity of the lower-latitude sea ice edge to the core of the eddy-driven jet (Chavaillaz et al. 2013; Sime et al. 2016).

In terms of future projections, a key point is that approximately half of the variance in projected twenty-first-century westerly jet strength response across the CMIP5 models is correlated with model-simulated historical sea ice area, which is an observable variable. This raises the question of whether differences between simulated and observed climatological SIA (e.g., see vertical dashed lines in Figs. 3a,e) could be used to provide an observational constraint on future projections of the westerly jet (i.e., an ''emergent constraint''; see Collins et al. 2012). However, to develop

confidence in such an approach, it will be important to better understand the drivers of present-day sea ice biases and diversity in projected responses. The comparison between atmosphere-only and coupled simulations conducted here suggests a coupled feedback between historical jet strength and future response. Specifically, atmospheric components of the CMIP5 models with a weaker westerly jet consequently exhibit a smaller SIA in coupled mode; less retreat of sea ice is therefore possible under future warming scenarios giving weaker polar amplification and stronger jet strengthening.

With regard to the first step in the above suggested coupled feedback (i.e., the cross-model link between mean-state SIA and JSTR), Fig. 9a closely reflects the results of Mahlstein et al. (2013), who evaluated cross-model links in the CMIP5 models between coupled mean-state sea ice area and coupled surface westerly wind strength south of 55°S. Their suggested mechanism for this relationship is that stronger surface westerlies cause a faster Ekman transport of the sea ice to the north by the Coriolis force and therefore more expansive sea ice. This is in agreement with the interpretation of Landrum et al. (2012) in their evaluation of the CMIP5 model with the second-largest mean-state annual-mean SIA of those assessed here (CCSM4). They also concluded that atmospheric circulation biases are key. Specifically, in CCSM4 the westerly wind stress bias is more than 30% larger than reanalysis products between 50° and 60°S, which is coincident with too-large equatorward sea ice transport and cool Southern Ocean SSTs.

This clear cross-model correlation between stronger westerlies and more sea ice is less robust in studies of transient responses to wind forcing [e.g., southern annular mode (SAM) index increases associated with the ozone hole formation], which in some climate models emerge as long-term SIA increases and in others emerge as SIA decreases (Sigmond and Fyfe 2010; Bitz and Polvani 2012; Smith et al. 2012; Purich et al. 2016; Holland et al. 2017; Kostov et al. 2017). The intermodel differences appear to be associated with a balance between equatorward Ekman transport (which is generally dominant on shorter annual–decadal time scales) acting to decrease Southern Ocean SSTs and increase SIA and upward Ekman pumping of warmer subsurface waters acting to increase SSTs and reduce SIA (which in approximately half of CMIP5 models emerges as dominant on longer time scales) (Ferreira et al. 2015; Holland et al. 2017; Kostov et al. 2017).

One possible reason for the less consistent results in the studies on transient responses to SAM/westerly anomaly forcing compared to studies on mean-state biases is that differences in mean-state JSTR are considerably larger in amplitude (a range of approximately $4\,\mathrm{m\,s^{-1}}$ in annual-mean JSTR across the AMIP models; see Fig. 9c) than the wind anomalies associated with the ozone hole [summer-only, near-surface jet strength perturbations of $\sim 0.3\,\mathrm{m\,s^{-1}}$ over three decades (e.g., Bracegirdle et al. 2013)]. With comparatively large differences in zonal wind profile, it is possible that Ekman transport plays a more important role than Ekman pumping or that the differing seasonality leads to a differing role for Ekman pumping. However, these suggestions will need to be considered in further research in which it will be essential to understand the different but interrelated roles of heat and momentum fluxes in driving mean-state SST and sea ice biases.

Although the AMIP–CMIP5 comparisons can help to identify causality, there is clearly further research required into linkages between sea ice, the broader Southern Ocean system, and atmospheric circulation. Key questions are as follows:

1) Do models that closely replicate observed SIA do so for the right reasons? [Current research comparing observed and simulated sea ice budgets indicates that this may not be the case (e.g., Uotila et al. 2014).]
2) To what extent do SIA-related proximal Southern Ocean surface conditions contribute to coupled interactions with the westerly jet?

In summary, many drivers of diversity in projections of SH circulation have been suggested in the literature, such as shortwave radiative forcing (associated with clouds; Ceppi et al. 2014), biases in atmospheric jet latitude (which affects eddy feedbacks; Chen and Held 2007; Barnes and Hartmann 2010; Simpson et al. 2012), and related biases in jet variability (which are important in relation to fluctuation–dissipation theory; Kidston and Gerber 2010; McGraw and Barnes 2016). All likely play a role in the fully coupled CMIP5 multimodel ensemble. The results shown here emphasize the potential importance of coupled baseline biases in SIA and westerly jet strength as a key source of diversity in CMIP5 jet responses under future climate change scenarios. This raises the possibility of developing observational constraints on future projections of winds over the Southern Ocean.

Acknowledgments. Three anonymous reviewers are thanked for their suggested improvements to the manuscript. The World Climate Research Programme's Working Group on Coupled Modelling, which is responsible for CMIP, and the climate modeling groups (listed in the appendix of this paper) are thanked for

producing and making available their model output. For CMIP, the U.S. Department of Energy's Program for Climate Model Diagnosis and Intercomparison provides coordinating support and led development of software infrastructure in partnership with the Global Organization for Earth System Science Portals. The original CMIP5 data can be accessed through the ESGF data portals (see http://pcmdi-cmip.llnl.gov/cmip5/availability.html). The European Centre for Medium-Range Weather Forecasts is thanked for providing the ERA-Interim dataset. This study was funded partially by the Natural Environment Research Council both as part of the British Antarctic Survey Polar Science for Planet Earth Programme and Grant NE/N018486/1. It was also funded by the Research Council of Norway as a contribution to Project 248803/E10. The Antarctic Climate Change in the 21st Century (AntClim21) Scientific Research Programme of the Scientific Committee on Antarctic Research are thanked for supporting a workshop at which early ideas for this study were initiated. ColorBrewer are acknowledged for providing the color scale used in the figures.

APPENDIX

Additional Information on the CMIP5 Models

The purpose of this appendix is to provide additional information on the CMIP5 models and the modeling center acronyms. More precise listings of the realizations used for each CMIP5 variable and model are shown in the tables of the supplemental material (Tables S1–S3).

BCC	Beijing Climate Center, China Meteorological Administration
CCCma	Canadian Centre for Climate Modelling and Analysis
CMCC	Centro Euro-Mediterraneo per I Cambiamenti Climatici
CNRM–CERFACS	Centre National de Recherches Météorologiques–Centre Européen de Recherche et de Formation Avancées en Calcul Scientifique
CSIRO–BoM	Commonwealth Scientific and Industrial Research Organisation (CSIRO) and Bureau of Meteorology (BoM)
CSIRO–QCCCE	Commonwealth Scientific and Industrial Research Organisation in collaboration with the Queensland Climate Change Centre of Excellence (QCCCE)
EC-EARTH	EC-EARTH consortium
FIO	First Institute of Oceanography, State Oceanic Administration (SOA)
GCESS	College of Global Change and Earth System Science, Beijing Normal University
INM	Institute of Numerical Mathematics
IPSL	L'Institut Pierre-Simon Laplace
LASG–CESS	LASG, Institute of Atmospheric Physics, Chinese Academy of Sciences; and Center for Earth System Science (CESS), Tsinghua University
MIROC (for MIROC5)	Atmosphere and Ocean Research Institute (The University of Tokyo), National Institute for Environmental Studies, and JAMSTEC
MIROC (for MIROC-ESM-CHEM)	JAMSTEC, Atmosphere and Ocean Research Institute (The University of Tokyo), and National Institute for Environmental Studies
MOHC	Met Office Hadley Centre
MPI-M	Max Planck Institute for Meteorology
MRI	Meteorological Research Institute
NASA GISS	NASA Goddard Institute for Space Studies
NCAR	National Center for Atmospheric Research
NCC	Norwegian Climate Centre
NIMR/KMA	National Institute of Meteorological Research/Korea Meteorological Administration
NOAA/GFDL	NOAA/Geophysical Fluid Dynamics Laboratory
NSF–DOE–NCAR	National Science Foundation, U.S. Department of Energy, and National Center for Atmospheric Research

REFERENCES

Bader, J., M. Flügge, N. G. Kvamstø, M. D. S. Mesquita, and A. Voigt, 2013: Atmospheric winter response to a projected future Antarctic sea-ice reduction: A dynamical analysis. *Climate Dyn.*, **40**, 2707–2718, doi:10.1007/s00382-012-1507-9.

Baker, H. S., T. Woollings, and C. Mbengue, 2017: Eddy-driven jet sensitivity to diabatic heating in an idealized GCM. *J. Climate*, **30**, 6413–6431, doi:10.1175/JCLI-D-16-0864.1.

Barnes, E. A., and D. L. Hartmann, 2010: Testing a theory for the effect of latitude on the persistence of eddy-driven jets using CMIP3 simulations. *Geophys. Res. Lett.*, **37**, L15801, doi:10.1029/2010GL044144.

Bitz, C. M., and L. M. Polvani, 2012: Antarctic climate response to stratospheric ozone depletion in a fine resolution ocean

climate model. *Geophys. Res. Lett.*, **39**, L20705, doi:10.1029/2012GL053393.

Bracegirdle, T. J., W. M. Connolley, and J. Turner, 2008: Antarctic climate change over the twenty first century. *J. Geophys. Res*, **113**, D03103, doi:10.1029/2007JD008933.

——, E. Shuckburgh, J.-B. Sallee, Z. Wang, A. J. S. Meijers, N. Bruneau, T. Phillips, and L. J. Wilcox, 2013: Assessment of surface winds over the Atlantic, Indian, and Pacific Ocean sectors of the Southern Ocean in CMIP5 models: Historical bias, forcing response, and state dependence. *J. Geophys. Res. Atmos.*, **118**, 547–562, doi:10.1002/jgrd.50153.

——, D. B. Stephenson, J. Turner, and T. Phillips, 2015: The importance of sea ice area biases in 21st century multimodel projections of Antarctic temperature and precipitation. *Geophys. Res. Lett.*, **42**, 10 832–10 839, doi:10.1002/2015GL067055.

Brayshaw, D. J., B. Hoskins, and M. Blackburn, 2011: The basic ingredients of the North Atlantic storm track. Part II: Sea surface temperatures. *J. Atmos. Sci.*, **68**, 1784–1805, doi:10.1175/2011JAS3674.1.

Ceppi, P., M. D. Zelinka, and D. L. Hartmann, 2014: The response of the Southern Hemispheric eddy-driven jet to future changes in shortwave radiation in CMIP5. *Geophys. Res. Lett.*, **41**, 3244–3250, doi:10.1002/2014GL060043.

Chavaillaz, Y., F. Codron, and M. Kageyama, 2013: Southern westerlies in LGM and future (RCP4.5) climates. *Climate Past*, **9**, 517–524, doi:10.5194/cp-9-517-2013.

Chen, G., and I. M. Held, 2007: Phase speed spectra and the recent poleward shift of Southern Hemisphere surface westerlies. *Geophys. Res. Lett.*, **34**, L21805, doi:10.1029/2007GL031200.

Collins, M., R. E. Chandler, P. M. Cox, J. M. Huthnance, J. Rougier, and D. B. Stephenson, 2012: Quantifying future climate change. *Nat. Climate Change*, **2**, 403–409, doi:10.1038/nclimate1414.

——, and Coauthors, 2013: Long-term climate change: Projections, commitments and irreversibility. *Climate Change 2013: The Physical Science Basis*, T. F. Stocker et al., Eds., Cambridge University Press, 1029–1136.

Comiso, J. C., 2000: Bootstrap sea ice concentrations from Nimbus-7 SMMR and DMSP SSM/I-SSMIS, version 2. National Snow and Ice Data Center, updated 2015, accessed 2016, http://nsidc.org/data/docs/daac/nsidc0079_bootstrap_seaice.gd.html.

Dee, D. P., and Coauthors, 2011: The ERA-Interim reanalysis: Configuration and performance of the data assimilation system. *Quart. J. Roy. Meteor. Soc.*, **137**, 553–597, doi:10.1002/qj.828.

Eisenman, I., 2010: Geographic muting of changes in the Arctic sea ice cover. *Geophys. Res. Lett.*, **37**, L16501, doi:10.1029/2010GL043741.

Eyring, V., and Coauthors, 2013: Long-term ozone changes and associated climate impacts in CMIP5 simulations. *J. Geophys. Res. Atmos.*, **118**, 5029–5060, doi:10.1002/jgrd.50316.

Ferreira, D., J. Marshall, C. M. Bitz, S. Solomon, and A. Plumb, 2015: Antarctic Ocean and sea ice response to ozone depletion: A two-time-scale problem. *J. Climate*, **28**, 1206–1226, doi:10.1175/JCLI-D-14-00313.1.

Flato, G., 2004: Sea-ice and its response to CO_2 forcing as simulated by global climate models. *Climate Dyn.*, **23**, 229–241, doi:10.1007/s00382-004-0436-7.

Frierson, D. M. W., 2006: Robust increases in midlatitude static stability in simulations of global warming. *Geophys. Res. Lett.*, **33**, L24816, doi:10.1029/2006GL027504.

Frölicher, T. L., J. L. Sarmiento, D. J. Paynter, J. P. Dunne, J. P. Krasting, and M. Winton, 2015: Dominance of the Southern Ocean in anthropogenic carbon and heat uptake in CMIP5 models. *J. Climate*, **28**, 862–886, doi:10.1175/JCLI-D-14-00117.1.

Gerber, E. P., and S. W. Son, 2014: Quantifying the summertime response of the austral jet stream and Hadley cell to stratospheric ozone and greenhouse gases. *J. Climate*, **27**, 5538–5559, doi:10.1175/JCLI-D-13-00539.1.

Grise, K. M., and L. M. Polvani, 2016: Is climate sensitivity related to dynamical sensitivity? *J. Geophys. Res. Atmos.*, **121**, 5159–5176, doi:10.1002/2015JD024687.

Hall, A., and M. Visbeck, 2002: Synchronous variability in the Southern Hemisphere atmosphere, sea ice, and ocean resulting from the Annular Mode. *J. Climate*, **15**, 3043–3057, doi:10.1175/1520-0442(2002)015<3043:SVITSH>2.0.CO;2.

Harvey, B. J., L. C. Shaffrey, and T. J. Woollings, 2014: Equator-to-pole temperature differences and the extra-tropical storm track responses of the CMIP5 climate models. *Climate Dyn.*, **43**, 1171–1182, doi:10.1007/s00382-013-1883-9.

——, ——, and ——, 2015: Deconstructing the climate change response of the Northern Hemisphere wintertime storm tracks. *Climate Dyn.*, **45**, 2847–2860, doi:10.1007/s00382-015-2510-8.

Held, I. M., 1993: Large-scale dynamics and global warming. *Bull. Amer. Meteor. Soc.*, **74**, 228–241, doi:10.1175/1520-0477(1993)074<0228:LSDAGW>2.0.CO;2.

Holland, M. M., and C. M. Bitz, 2003: Polar amplification of climate change in coupled models. *Climate Dyn.*, **21**, 221–232, doi:10.1007/s00382-003-0332-6.

——, L. Landrum, Y. Kostov, and J. Marshall, 2017: Sensitivity of Antarctic sea ice to the Southern Annular Mode in coupled climate models. *Climate Dyn.*, **49**, 1813–1831, doi:10.1007/s00382-016-3424-9.

Kidston, J., and E. P. Gerber, 2010: Intermodel variability of the poleward shift of the austral jet stream in the CMIP3 integrations linked to biases in 20th century climatology. *Geophys. Res. Lett.*, **37**, L09708, doi:10.1029/2010GL042873.

——, A. S. Taschetto, D. W. J. Thompson, and M. H. England, 2011: The influence of Southern Hemisphere sea-ice extent on the latitude of the mid-latitude jet stream. *Geophys. Res. Lett.*, **38**, L15804, doi:10.1029/2011GL048056.

Kostov, Y., J. Marshall, U. Hausmann, K. C. Armour, D. Ferreira, and M. M. Holland, 2017: Fast and slow responses of Southern Ocean sea surface temperature to SAM in coupled climate models. *Climate Dyn.*, **48**, 1595–1609, doi:10.1007/s00382-016-3162-z.

Krinner, G., C. Largeron, M. Ménégoz, C. Agosta, and C. Brutel-Vuilmet, 2014: Oceanic forcing of Antarctic climate change: A study using a stretched-grid atmospheric general circulation model. *J. Climate*, **27**, 5786–5800, doi:10.1175/JCLI-D-13-00367.1.

Kushner, P. J., I. M. Held, and T. L. Delworth, 2001: Southern Hemisphere atmospheric circulation response to global warming. *J. Climate*, **14**, 2238–2249, doi:10.1175/1520-0442(2001)014<0001:SHACRT>2.0.CO;2.

Landrum, L., M. M. Holland, D. P. Schneider, and E. Hunke, 2012: Antarctic sea ice climatology, variability, and late twentieth-century change in CCSM4. *J. Climate*, **25**, 4817–4838, doi:10.1175/JCLI-D-11-00289.1.

Le Quéré, C., and Coauthors, 2007: Saturation of the Southern Ocean CO_2 sink due to recent climate change. *Science*, **316**, 1735–1738, doi:10.1126/science.1136188.

Lorenz, D. J., and E. T. DeWeaver, 2007: Tropopause height and zonal wind response to global warming in the IPCC scenario integrations. *J. Geophys. Res.*, **112**, D10119, doi:10.1029/2006JD008087.

Lovenduski, N. S., N. Gruber, S. C. Doney, and I. D. Lima, 2007: Enhanced CO_2 outgassing in the Southern Ocean from a positive phase of the Southern Annular Mode. *Global Biogeochem. Cycles*, **21**, GB2026, doi:10.1029/2006GB002900.

Mahlstein, I., P. R. Gent, and S. Solomon, 2013: Historical Antarctic mean sea ice area, sea ice trends, and winds in CMIP5 simulations. *J. Geophys. Res. Atmos.*, **118**, 5105–5110, doi:10.1002/jgrd.50443.

McGraw, M. C., and E. A. Barnes, 2016: Seasonal sensitivity of the eddy-driven jet to tropospheric heating in an idealized AGCM. *J. Climate*, **29**, 5223–5240, doi:10.1175/JCLI-D-15-0723.1.

Meijers, A. J. S., E. Shuckburgh, N. Bruneau, J. B. Sallee, T. J. Bracegirdle, and Z. Wang, 2012: Representation of the Antarctic Circumpolar Current in the CMIP5 climate models and future changes under warming scenarios. *J. Geophys. Res.*, **117**, C12008, doi:10.1029/2012JC008412.

Meinshausen, M., and Coauthors, 2011: The RCP greenhouse gas concentrations and their extensions from 1765 to 2300. *Climatic Change*, **109**, 213–241, doi:10.1007/s10584-011-0156-z.

Meredith, M. P., and A. M. Hogg, 2006: Circumpolar response of Southern Ocean eddy activity to a change in the Southern Annular Mode. *Geophys. Res. Lett.*, **33**, L16608, doi:10.1029/2006GL026499.

Purich, A., W. J. Cai, M. H. England, and T. Cowan, 2016: Evidence for link between modelled trends in Antarctic sea ice and underestimated westerly wind changes. *Nat. Commun.*, **7**, 10409, doi:10.1038/ncomms10409.

Raphael, M. N., 2003: Impact of observed sea-ice concentration on the Southern Hemisphere extratropical atmospheric circulation in summer. *J. Geophys. Res.*, **108**, 4687, doi:10.1029/2002JD003308.

Rivière, G., 2011: A dynamical interpretation of the poleward shift of the jet streams in global warming scenarios. *J. Atmos. Sci.*, **68**, 1253–1272, doi:10.1175/2011JAS3641.1.

Sallee, J. B., E. Shuckburgh, N. Bruneau, A. J. S. Meijers, T. J. Bracegirdle, Z. Wang, and T. Roy, 2013: Assessment of Southern Ocean water mass circulation and characteristics in CMIP5 models: Historical bias and forcing response. *J. Geophys. Res. Oceans*, **118**, 1830–1844, doi:10.1002/jgrc.20135.

Sigmond, M., and J. C. Fyfe, 2010: Has the ozone hole contributed to increased Antarctic sea ice extent? *Geophys. Res. Lett.*, **37**, L18502, doi:10.1029/2010GL044301.

Sime, L. C., K. E. Kohfeld, C. Le Quéré, E. W. Wolff, A. M. de Boer, R. M. Graham, and L. Bopp, 2013: Southern Hemisphere westerly wind changes during the Last Glacial Maximum: Model–data comparison. *Quat. Sci. Rev.*, **64**, 104–120, doi:10.1016/j.quascirev.2012.12.008.

——, D. Hodgson, T. J. Bracegirdle, C. Allen, B. Perren, S. Roberts, and A. M. de Boer, 2016: Sea ice led to poleward-shifted winds at the Last Glacial Maximum: The influence of state dependency on CMIP5 and PMIP3 models. *Climate Past*, **12**, 2241–2253, doi:10.5194/cp-12-2241-2016.

Simpson, I. R., and L. M. Polvani, 2016: Revisiting the relationship between jet position, forced response, and annular mode variability in the southern midlatitudes. *Geophys. Res. Lett.*, **43**, 2896–2903, doi:10.1002/2016GL067989.

——, M. Blackburn, and J. D. Haigh, 2012: A mechanism for the effect of tropospheric jet structure on the annular mode–like response to stratospheric forcing. *J. Atmos. Sci.*, **69**, 2152–2170, doi:10.1175/JAS-D-11-0188.1.

Smith, K. L., L. M. Polvani, and D. R. Marsh, 2012: Mitigation of 21st century Antarctic sea ice loss by stratospheric ozone recovery. *Geophys. Res. Lett.*, **39**, L20701, doi:10.1029/2012GL053325.

Taylor, K. E., R. J. Stouffer, and G. A. Meehl, 2012: An overview of CMIP5 and the experiment design. *Bull. Amer. Meteor. Soc.*, **93**, 485–498, doi:10.1175/BAMS-D-11-00094.1.

Uotila, P., P. R. Holland, T. Vihma, S. J. Marsland, and N. Kimura, 2014: Is realistic Antarctic sea-ice extent in climate models the result of excessive ice drift? *Ocean Modell.*, **79**, 33–42, doi:10.1016/j.ocemod.2014.04.004.

Waugh, D. W., F. Primeau, T. DeVries, and M. Holzer, 2013: Recent changes in the ventilation of the southern oceans. *Science*, **339**, 568–570, doi:10.1126/science.1225411.

Wilcox, L. J., A. J. Charlton-Perez, and L. J. Gray, 2012: Trends in Austral jet position in ensembles of high- and low-top CMIP5 models. *J. Geophys. Res.*, **117**, D13115, doi:10.1029/2012JD017597.

Williams, G. P., 2006: Circulation sensitivity to tropopause height. *J. Atmos. Sci.*, **63**, 1954–1961, doi:10.1175/JAS3762.1.

Wittman, M. A. H., A. J. Charlton, and L. M. Polvani, 2007: The effect of lower stratospheric shear on baroclinic instability. *J. Atmos. Sci.*, **64**, 479–496, doi:10.1175/JAS3828.1.

Woollings, T., L. Papritz, C. Mbengue, and T. Spengler, 2016: Diabatic heating and jet stream shifts: A case study of the 2010 negative North Atlantic Oscillation winter. *Geophys. Res. Lett.*, **43**, 9994–10 002, doi:10.1002/2016GL070146.

Yin, J. H., 2005: A consistent poleward shift of the storm tracks in simulations of 21st century climate. *Geophys. Res. Lett.*, **32**, L18701, doi:10.1029/2005GL023684.